Available online at www.sciencedirect.com
SCIENCE DIRECT®
Journal of Organometallic Chemistry 671 (2003) 158–165
Journal of Organometallic Chemistry
www.elsevier.com/locate/jorganchem

Facile introduction of bridging MPh_2 groups (M=Ge, Sn, Pb) into platinum–pentaruthenium and hexaruthenium carbido carbonyl cluster complexes

Richard D. Adams *, Burjor Captain, Wei Fu

Department of Chemistry and Biochemistry, USC NanoCenter, University of South Carolina, Columbia, SC 29208, USA

Received 9 December 2002; received in revised form 30 January 2003; accepted 30 January 2003

Abstract

The reactions of $PtRu_5(CO)_{16}(\mu_6\text{-C})$ (**1**) with Ph_3GeH and Ph_3SnH afforded the trimetallic cluster complexes $PtRu_5(CO)_{15}(\mu\text{-}GePh_2)(\mu_6\text{-C})$ (**4**) and $PtRu_5(CO)_{15}(\mu\text{-}SnPh_2)(\mu_6\text{-C})$ (**5**), respectively, in good yields. Both the compounds consist of an octahedral cluster of one platinum and five ruthenium atoms with an interstitial carbido ligand in the center. The bridging CO ligand in **1** was replaced by a bridging $GePh_2$ group in **4** and a bridging $SnPh_2$ group in **5**. The lead homologue $PtRu_5(CO)_{15}(\mu\text{-}PbPh_2)(\mu_6\text{-C})$ (**6**) was obtained from the reaction of **1** with Pb_2Ph_6. The reaction of $PtRu_5(CO)_{15}(PMe_2Ph)(\mu_6\text{-C})$ (**2**) with Ph_3SnH yielded the phosphine derivative of **5**, $PtRu_5(CO)_{14}(\mu\text{-}SnPh_2)(PMe_2Ph)(\mu_6\text{-C})$ (**7**). Compound **7** was obtained in a higher yield from the reaction of **5** with PMe_2Ph. The reaction of $Ru_6(CO)_{14}(\eta^6\text{-}C_6H_6)(\mu_6\text{-C})$ (**3**) with Ph_3SnH yielded the new hexaruthenium complex $Ru_6(CO)_{13}(\mu\text{-}SnPh_2)(\eta^6\text{-}C_6H_6)(\mu_6\text{-C})$ (**8**) containing a bridging $SnPh_2$ ligand. Evidence for benzene formation in the formation of compound **5** indicates the fate of the phenyl group that was cleaved from the tin atom in that reaction.

Keywords: Ruthenium; Platinum; Germanium; Tin; Lead; Trimetallic cluster

1. Introduction

Recent studies have shown that bimetallic nanoparticles can be prepared from bimetallic molecular cluster precursors [1–8]. Bimetallic nanoparticles have been shown to exhibit superior catalytic activity under heterogeneous conditions [8,9]. Germanium, tin, and lead have been shown to be important modifiers for transition metal catalysts on supports for a variety of reactions including the important naphtha reforming process [10–13]. Ruthenium catalysts combined with the Group 14 elements, germanium, tin, or lead, have also been found to exhibit interesting catalytic properties [14–16]. There is extensive literature on transition metal complexes containing Group 14 elements [17–20]; however, there are only a few examples of molecular ruthenium–germanium cluster complexes [21–23]. We have recently reported that triphenylgermane and triphenylstannane react with pentaruthenium carbido carbonyl cluster complexes to yield bimetallic clusters containing as many as four and five bridging diphenylgermyl and diphenylstannyl ligands [24,25]. These ligands were formed by the cleavage of phenyl groups from intermediate complexes containing triphenyltin ligands.

We have now found that we can obtain complexes containing bridging diphenylgermyl, diphenylstannyl, and diphenylplumbyl ligands from the reactions of Ph_3GeH, Ph_3SnH, and Pb_2Ph_6 with the hexanuclear cluster complex $PtRu_5(CO)_{16}(\mu_6\text{-C})$ (**1**) [26]. The reactions of Ph_3SnH with $PtRu_5(CO)_{15}(PMe_2Ph)(\mu_6\text{-C})$ (**2**) [27] and $Ru_6(CO)_{14}(\eta^6\text{-}C_6H_6)(\mu_6\text{-C})$ (**3**) [28] were also investigated and yielded similar products containing bridging $SnPh_2$ ligands. These results are described in this report.

* Corresponding author. Tel.: +1-803-7777187; fax: +1-803-7776781.
E-mail address: adams@mail.chem.sc.edu (R.D. Adams).

0022-328X/03/$ - see front matter © 2003 Elsevier Science B.V. All rights reserved.
doi:10.1016/S0022-328X(03)00099-8

2. Experimental

2.1. General data

All reactions were performed under a nitrogen atmosphere. Reagent grade solvents were dried by the standard procedures and were freshly distilled prior to use. Infrared spectra were recorded on a Nicolet 5DXBO and an Avatar 360 FTIR spectrophotometer. ^{1}H-NMR spectra were recorded on a Varian Inova 300 spectrometer operating at 300.08 MHz. Elemental analyses were performed by Desert Analytics (Tucson, AZ). Ph_3SnH and $Ph_3Pb_2Ph_3$ were purchased from Alfa Products and Ph_3GeH was purchased from Gelest, and were used without further purification. $PtRu_5(CO)_{16}(\mu_6$-C) (**1**) [26], $PtRu_5(CO)_{15}(PMe_2Ph)(\mu_6$-C) (**2**) [27], and $Ru_6(CO)_{14}(\eta^6$-$C_6H_6)(\mu_6$-C) (**3**) [28] were prepared according to the published procedures. Product separations were performed by TLC in air on Analtech 0.25 and 0.5 mm silica gel 60 Å F_{254} glass plates.

2.2. Reaction of $PtRu_5(CO)_{16}(\mu_6$-C) with Ph_3GeH

18.0 mg of **1** (0.016 mmol) and 5 mg of Ph_3GeH (0.016 mmol) were dissolved in 30 ml of hexane in a 50-ml three-neck round-bottomed flask equipped with a stir bar. The reaction mixture was then heated to reflux for 2 h. After cooling, the solvent was removed in vacuo, and the product was isolated by TLC on silica gel by using pure hexane to yield 14 mg (67%) of red $PtRu_5(CO)_{15}(\mu$-$GePh_2)(\mu_6$-C) (**4**). Spectral data for **4**: IR ν_{CO} (cm^{-1} in hexane): 2091 (w), 2061 (vs), 2045 (vs), 2030 (m), 2023 (w, sh), 1993 (w). ^{1}H-NMR (CD_2Cl_2): $\delta = 7.46$–7.56 (m, 10H). Anal. Calc.: C, 24.74; H, 0.74. Found: C, 24.84; H, 0.72%.

2.3. Reaction of $PtRu_5(CO)_{16}(\mu_6$-C) with Ph_3SnH

14.8 mg of **1** (0.013 mmol) was dissolved in 50 ml hexane in a 100-ml three-neck round-bottomed flask equipped with a stir bar. To this solution, 4.5 mg of Ph_3SnH (0.013 mmol) dissolved in 5 ml hexane was added and allowed to stir at room temperature (r.t.) for 10 min. The reaction mixture was concentrated to about 5 ml and was then placed in the freezer at -80 °C for overnight. This yielded 14 mg of $PtRu_5(CO)_{15}(\mu$-$SnPh_2)(\mu_6$-C) (**5**) (78%) in the form of a red powder. Note: this compound decomposes when chromatographed on silica gel. Spectral data for **5**: IR ν_{CO} (cm^{-1} in hexane): 2090 (m), 2060 (vs), 2043 (vs), 2031 (m), 2021 (m), 1992 (w), 1973 (w). ^{1}H-NMR (CD_2Cl_2): $\delta = 7.46$–7.70 (m, 10H). Anal. Calc.: C, 23.93; H, 0.74. Found: C, 23.87; H, 0.84%. When the reaction was performed in an NMR tube using CD_2Cl_2 solvent, the ^{1}H-NMR spectrum of the reaction mixture showed the resonances for compound **5** and a single resonance ($\delta =$ 7.37 ppm) that is attributed to benzene within 15 min.

2.4. Reaction of $PtRu_5(CO)_{16}(\mu_6$-C) with Pb_2Ph_6

17.3 mg of **1** (0.015 mmol) and 26.3 mg of Pb_2Ph_6 (0.030 mmol) were dissolved in 40 ml of hexane in a 100-ml three-neck round-bottomed flask equipped with a stir bar. The reaction mixture was then heated to reflux for 2 h. After cooling, the solvent was removed in vacuo, and the product was isolated by TLC on silica gel by using a 3:1 hexane–methylene chloride solvent mixture to yield 9 mg (40%) of red $PtRu_5(CO)_{15}(\mu$-$PbPh_2)(\mu_6$-C) (**6**). Spectral data for **6**: IR ν_{CO} (cm^{-1} in hexane): 2089 (w), 2058 (vs), 2042 (vs), 2030 (w, sh), 2021 (w, sh), 1995 (vw). ^{1}H-NMR (CD_2Cl_2): $\delta = 7.46$–8.05 (m, 10H). Anal. Calc.: C, 22.51; H, 0.67. Found: C, 22.74; H, 0.76%.

2.5. Reaction of $PtRu_5(CO)_{15}(PMe_2Ph)(\mu_6$-C) with Ph_3SnH

10.5 mg of **2** (0.008 mmol) was dissolved in 25 ml of hexane in a 50-ml three-neck round-bottomed flask equipped with a stir bar. To this solution, 2.9 mg of Ph_3SnH (0.008 mmol) dissolved in 5 ml of hexane was added. The reaction mixture was then brought to reflux for 2 h. After cooling, the solvent was removed in vacuo, and the product was separated by TLC using a 2:1 hexane–methylene chloride solvent mixture to yield 2.7 mg (20%) of a red product, $PtRu_5(CO)_{14}(\mu$-$SnPh_2)$-$(PMe_2Ph)(\mu_6$-C) (**7**). Spectral data for **7**: IR ν_{CO} (cm^{-1} in hexane): 2076 (s), 2047 (vs), 2027 (vs), 1976 (m). ^{1}H-NMR (CD_2Cl_2): $\delta = 7.1$–7.6 (m, 15H), 1.96 (d, 6H, CH_3, $^2J_{P-H} = 10$ Hz, $^3J_{Pt-H} = 47$ Hz). Anal. Calc.: C, 27.74; H, 1.40. Found: C, 28.03; H, 1.43%.

2.6. Reaction of **5** with PMe_2Ph

10.0 mg of **5** (0.007 mmol) and 1 μl of PMe_2Ph (0.006 mmol) were dissolved in 25 ml of hexane in a 50-ml three-neck round-bottomed flask equipped with a stir bar. The reaction mixture was then heated to reflux for 2 h. After cooling, the solvent was removed in vacuo, and the product was separated by TLC by using a 2:1 hexane–methylene chloride solvent mixture to yield 4.4 mg (41%) of **7**.

2.7. Reaction of $Ru_6(CO)_{14}(\eta^6$-$C_6H_6)(\mu_6$-C) with Ph_3SnH

13.4 mg (0.012 mmol) of **3** was dissolved in 10 ml CH_2Cl_2 in a 50-ml three-neck round-bottomed flask equipped with a stir bar. To this solution, 16 mg (0.045 mmol) of Ph_3SnH dissolved in 10 ml of CH_2Cl_2 was added. The reaction mixture was allowed to stir for 16 h

Table 1
Crystallographic data for compounds **4**, **5**, and **6**

	4	**5**	**6**
Empirical formula	$PtRu_5GeO_{15}C_{28}H_{10}$	$PtRu_5SnO_{15}C_{28}H_{10}$	$PtRu_5PbO_{15}C_{28}H_{10}$
Formula weight	1359.41	1405.51	1493.99
Crystal system	Triclinic	Triclinic	Triclinic
Lattice parameters			
a (Å)	12.4804(12)	12.711(1)	12.7357(6)
b (Å)	14.8564(24)	14.816(2)	14.7776(7)
c (Å)	9.7642(19)	9.793(1)	9.7778(5)
α (°)	101.208(14)	102.12(1)	77.3970(10)
β (°)	93.698(13)	93.621(9)	86.4230(10)
γ (°)	79.498(11)	79.12(1)	79.0480(10)
V (Å^3)	1745.3(5)	1770.3(4)	1762.74(15)
Space group	$P\bar{1}$	$P\bar{1}$	$P\bar{1}$
Z-value	2	2	2
ρ_{calc} (g cm^{-3})	2.587	2.637	2.815
μ (Mo–K$_\alpha$) (mm^{-1})	6.997	6.755	10.860
Temperature (K)	293	293	293
$2\Theta_{max}$ (°)	43.98	44.0	56.64
Number of observations	3956 ($I > 3\sigma(I)$)	3913 ($I > 3\sigma(I)$)	6930 ($I > 2\sigma(I)$)
Number of parameters	452	452	451
Goodness of fit	1.052	1.021	1.006
Maximum shift in cycle	0.001	0.007	0.001
Residuals [a]: R_1; wR_2	0.0220; 0.0359	0.0312; 0.0437	0.0364; 0.0697
Absorption correction	DIFABS	DIFABS	SADABS
Max/min	1.00/0.74	1.00/0.44	1.00/0.70
Largest peak in final diff. map (e Å^{-3})	0.52	1.00	1.54

[a] $R = \Sigma_{hkl}(||F_{obs}| - |F_{calc}||)/\Sigma_{hkl}|F_{obs}|$; $R_w = [\Sigma_{hkl} w(|F_{obs}| - |F_{calc}|)^2/\Sigma_{hkl} wF_{obs}^2]^{1/2}$; $w = 1/\sigma^2(F_{obs})$; goodness of fit $= [\Sigma_{hkl} w(|F_{obs}| - |F_{calc}|)^2/(n_{data} - n_{vari})]^{1/2}$.

at r.t. The solvent was then removed in vacuo and separated by TLC using a 2:1 hexane–methylene chloride solvent mixture to yield 1.6 mg (10%) of a dark red product, $Ru_6(CO)_{13}(\mu\text{-}SnPh_2)(\eta^6\text{-}C_6H_6)(\mu_6\text{-}C)$ (**8**). Spectral data for **8**: IR ν_{CO} (cm^{-1} in CH_2Cl_2): 2069 (s), 2028 (s, sh), 2020 (vs), 1984 (m). ^{1}H-NMR ($CDCl_3$): $\delta = 7.3$–7.82 (m, 10H), 5.17 (s, 6H). Anal. Calc.: C, 28.82; H, 1.21. Found: C, 28.50; H, 1.35%.

2.8. Crystallographic analysis

Dark red crystals of **4**, **5**, **7**, and **8** suitable for diffraction analysis were grown by slow evaporation of solvent from solutions in hexane–methylene chloride solvent mixtures at 25 °C. Red crystals of **6** were grown by slow evaporation of solvent from solutions in hexane–methylene chloride solvent mixtures at −25 °C. For compounds **4**, **5**, and **8** the crystals used for the diffraction measurements were mounted in thin-walled glass capillaries. Diffraction measurements were made on a Rigaku AFC6S fully automated four-circle diffractometer using graphite-monochromated Mo–K$_\alpha$ radiation at 20 °C. The unit-cell was determined and refined from 15 randomly selected reflections obtained by using the AFC6 automatic search, center, index, and least-squares routines. All data processing were performed on a Silicon Graphic Indigo 2 computer by using the TEXSAN motif structure solving program library obtained from the Molecular Structure Corp., The Woodlands, TX. Neutral atom scattering factors were calculated by the standard procedures [29a]. Anomalous dispersion corrections were applied to all non-hydrogen atoms [29b]. Lorentz/polarization (Lp) and absorption corrections were applied to the data for each structure. Full-matrix least-squares refinements minimized the function $\Sigma_{hkl} w(|F_{obs}| - |F_{calc}|)^2$, where $w = 1/\sigma^2(F)$, $\sigma(F) = \sigma(F_{obs}^2)/2F_{obs}$, and $\sigma(F_{obs}^2) = [(\sigma I_{raw})^2 + (0.06 I_{net})^2]^{1/2}/\text{Lp}$. The structure was solved by a combination of direct methods (SIR 92) and difference Fourier syntheses.

For compounds **6** and **7** the data crystals were glued onto the end of a thin glass fiber. X-ray intensity data were measured using a Bruker SMART APEX CCD-based diffractometer using Mo–K$_\alpha$ radiation (λ = 0.71073 Å). The raw data frames were integrated with the SAINT+ program using a narrow-frame integration algorithm [30]. Correction for the Lorentz and polarization effects was also applied by SAINT. An empirical absorption correction based on the multiple measurement of equivalent reflections was applied by using the program SADABS. These structures were solved by a combination of direct methods and difference Fourier syntheses, and refined by full-matrix least-squares on F^2, using the SHELXTL software package [31]. Crystal data,

Table 2
Crystallographic data for compounds **7** and **8**

	7	**8**
Empirical formula	$PtRu_5SnPO_{14}C_{35}H_{21}$	$Ru_6SnO_{13}C_{32}H_{16}$
Formula weight	1515.62	1333.58
Crystal system	Monoclinic	Triclinic
Lattice parameters		
a (Å)	15.1624(18)	10.823(2)
b (Å)	17.983(2)	18.202(3)
c (Å)	15.3627(19)	10.747(3)
α (°)	90	103.81(2)
β (°)	97.689(3)	116.34(1)
γ (°)	90	85.65(1)
V (Å^3)	4151.1(9)	1841.4(7)
Space group	$P2_1/n$	$P\bar{1}$
Z-value	4	2
ρ_{calc} (g cm^{-3})	2.425	2.405
μ (Mo–K$_\alpha$) (mm^{-1})	5.819	3.124
Temperature (K)	293	293
$2\Theta_{max}$ (°)	52.8	44.0
Number of observations	6978 ($I > 2\sigma(I)$)	3027 ($I > 3\sigma(I)$)
Number of parameters	517	469
Goodness of fit	0.975	1.033
Maximum shift in cycle	0.002	0.00
Residuals [a]: R_1; wR_2	0.0337; 0.0774	0.0287; 0.0355
Absorption correction	SADABS	DIFABS
Max/min	0.26; 0.10	1.00; 0.75
Largest peak in final diff. map (e Å^{-3})	1.73	0.68

[a] $R = \Sigma_{hkl}(||F_{obs}| - |F_{calc}||)/\Sigma_{hkl}|F_{obs}|$; $R_w = [\Sigma_{hkl} w(|F_{obs}| - |F_{calc}|)^2/\Sigma_{hkl} wF_{obs}^2]^{1/2}$; $w = 1/\sigma^2(F_{obs})$; goodness of fit $= [\Sigma_{hkl} w(|F_{obs}| - |F_{calc}|)^2/(n_{data} - n_{vari})]^{1/2}$.

data collection parameters, and results of the analyses for compounds **4**, **5**, and **6** are listed in Table 1. For compounds **7** and **8**, this information is listed in Table 2.

Compounds **4**, **5**, and **8** were crystallized in the triclinic crystal system. The space group $P\bar{1}$ was assumed and confirmed by the successful solution and refinement of the structure. The structure was solved by a combination of direct methods (SIR 92) and difference Fourier syntheses. All non-hydrogen atoms were refined with anisotropic displacement parameters. The positions of the hydrogen atoms on the phenyl rings were calculated by assuming idealized geometries at the carbon atoms with C–H distances of 0.95 Å. The scattering contributions of these hydrogen atoms were included in the structure factor calculations, but their positions were not refined.

Compound **6** was crystallized in the triclinic crystal system. The space group $P\bar{1}$ was assumed and confirmed by the successful solution and refinement of the structure. The structure was solved by a combination of direct methods and difference Fourier syntheses, and refined by full-matrix least-squares on F^2, using the SHELXTL software package [31]. All non-hydrogen atoms were refined with anisotropic displacement parameters. Hydrogen atoms were placed in geometrically idealized positions and included as standard riding atoms.

Compound **7** was crystallized in the monoclinic crystal system. The space group $P2_1/n$ was identified uniquely on the basis of the systematic absences in the intensity data. The structure was solved by a combination of direct methods and difference Fourier syntheses, and refined by full-matrix least-squares on F^2, using the SHELXTL software package [31]. All non-hydrogen atoms were refined with anisotropic displacement parameters. Hydrogen atoms were placed in geometrically idealized positions and included as standard riding atoms.

3. Results and discussion

The reactions of $PtRu_5(CO)_{16}(\mu_6\text{-C})$ (**1**) with Ph_3GeH and Ph_3SnH afforded the trimetallic cluster complexes $PtRu_5(CO)_{15}(\mu\text{-}GePh_2)(\mu_6\text{-C})$ (**4**) and $PtRu_5(CO)_{15}(\mu\text{-}SnPh_2)(\mu_6\text{-C})$ (**5**) in 67 and 78% yields, respectively. The reaction with Ph_3SnH was complete within 10 min at room temperature, but the reaction with Ph_3GeH required heating to the reflux temperature of the hexane solvent for 2 h. Similarly, when heated to reflux in hexane solvent for 2 h, compound **1** reacted with Pb_2Ph_6 to give the lead homologue of **4** and **5**, $PtRu_5(CO)_{15}(\mu\text{-}PbPh_2)(\mu_6\text{-C})$ (**6**), in 40% yield. All the three compounds were characterized by a combination of IR, NMR, and single crystal X-ray diffraction analyses. All the three compounds are crystallographically isomorphous in the solid state, and the molecular structures of all the three compounds are similar. An ORTEP diagram representing the molecular structures of **4**–**6** is shown in Fig. 1, M = Ge, Sn, Pb. Selected bond distances and angles for all three structures are listed in Table 3. Each compound consists of an octahedral-shaped cluster of six metal

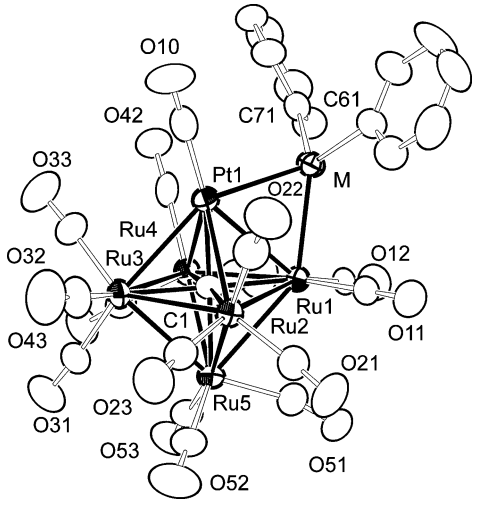

Fig. 1. An ORTEP diagram representing the molecular structures of the compounds **4**, **5**, and **6**, M = Ge, Sn, Pb.

Table 3
Selected intramolecular distances and angles for compounds **4**, **5**, and **6** [a]

Compound **4**		Compound **5**		Compound **6**	
Atom	Distance (Å)	Atom	Distance (Å)	Atom	Distance (Å)
Ru(1)–Pt(1)	2.8550(5)	Ru(1)–Pt(1)	2.9190(6)	Ru(1)–Pt(1)	2.9406(5)
Ru(1)–Ru(2)	2.9576(6)	Ru(1)–Ru(2)	2.9444(8)	Ru(1)–Ru(2)	2.9318(7)
Ru(1)–Ru(4)	2.9153(6)	Ru(1)–Ru(4)	2.9154(7)	Ru(1)–Ru(4)	2.9061(7)
Ru(1)–Ru(5)	2.9525(6)	Ru(1)–Ru(5)	2.9279(8)	Ru(1)–Ru(5)	2.8926(7)
Ru(2)–Pt(1)	2.9382(5)	Ru(2)–Pt(1)	2.9357(7)	Ru(2)–Pt(1)	2.9203(6)
Ru(2)–Ru(3)	2.9526(6)	Ru(2)–Ru(3)	2.9589(8)	Ru(2)–Ru(3)	2.9464(7)
Ru(2)–Ru(5)	2.8060(6)	Ru(2)–Ru(5)	2.8118(7)	Ru(2)–Ru(5)	2.8013(7)
Ru(3)–Pt(1)	2.9025(5)	Ru(3)–Pt(1)	2.8797(6)	Ru(3)–Pt(1)	2.8507(6)
Ru(3)–Ru(4)	2.8538(6)	Ru(3)–Ru(4)	2.8564(8)	Ru(3)–Ru(4)	2.8453(7)
Ru(3)–Ru(5)	2.9005(6)	Ru(3)–Ru(5)	2.8972(8)	Ru(3)–Ru(5)	2.8948(7)
Ru(4)–Ru(5)	2.8653(6)	Ru(4)–Ru(5)	2.8699(8)	Ru(4)–Ru(5)	2.8553(7)
Pt(1)–Ge(1)	2.4701(6)	Pt(1)–Sn(1)	2.6314(6)	Pt(1)–Pb(1)	2.7037(3)
Ru(1)–Ge(1)	2.4457(8)	Ru(1)–Sn(1)	2.6074(7)	Ru(1)–Pb(1)	2.6668(5)
Pt(1)–C(1)	2.051(5)	Pt(1)–C(1)	2.048(6)	Pt(1)–C(1)	2.040(5)
Ru(1)–C(1)	2.022(5)	Ru(1)–C(1)	2.040(7)	Ru(1)–C(1)	2.025(5)
Ru(2)–C(1)	2.100(5)	Ru(2)–C(1)	2.076(6)	Ru(2)–C(1)	2.067(5)
Ru(3)–C(1)	2.076(5)	Ru(3)–C(1)	2.069(7)	Ru(3)–C(1)	2.072(5)
Ru(4)–C(1)	2.058(5)	Ru(4)–C(1)	2.071(6)	Ru(4)–C(1)	2.061(5)
Ru(5)–C(1)	2.059(5)	Ru(5)–C(1)	2.060(6)	Ru(5)–C(1)	2.049(5)
C–O(av)	1.14(1)	C–O(av)	1.14(1)	C–O(av)	1.13(1)
Atom	Angle (°)	Atom	Angle (°)	Atom	Angle (°)
Ru(1)–Pt(1)–Ru(3)	90.22(2)	Ru(1)–Pt(1)–Ru(3)	90.22(2)	Ru(1)–Pt(1)–Ru(3)	90.020(15)
Ru(1)–Pt(1)–Sn(1)	57.75(2)	Ru(1)–Pt(1)–Sn(1)	57.75(2)	Ru(1)–Pt(1)–Pb(1)	56.200(12)
Pt(1)–Ru(1)–Sn(1)	56.53(2)	Pt(1)–Ru(1)–Sn(1)	56.53(2)	Pt(1)–Ru(1)–Pb(1)	57.406(12)
Pt(1)–Sn(1)–Ru(1)	67.72(2)	Pt(1)–Sn(1)–Ru(1)	67.72(2)	Pt(1)–Pb(1)–Ru(1)	66.394(12)
Ru(1)–Ru(5)–Ru(3)	89.70(2)	Ru(1)–Ru(5)–Ru(3)	89.70(2)	Ru(1)–Ru(5)–Ru(3)	90.111(19)
Ru(4)–Ru(5)–Ru(2)	93.55(2)	Ru(4)–Ru(5)–Ru(2)	93.55(2)	Ru(4)–Ru(5)–Ru(2)	93.53(2)
Pt(1)–Ru(1)–Ru(5)	89.20(2)	Pt(1)–Ru(1)–Ru(5)	89.20(2)	Pt(1)–Ru(1)–Ru(5)	88.919(17)
Pt(1)–Ru(3)–Ru(5)	90.58(2)	Pt(1)–Ru(3)–Ru(5)	90.58(2)	Pt(1)–Ru(3)–Ru(5)	90.648(17)
Ru(4)–Ru(1)–Ru(2)	89.91(2)	Ru(4)–Ru(1)–Ru(2)	89.91(2)	Ru(4)–Ru(1)–Ru(2)	89.812(19)
Ru(4)–Ru(3)–Ru(2)	90.77(2)	Ru(4)–Ru(3)–Ru(2)	90.77(2)	Ru(4)–Ru(3)–Ru(2)	90.711(19)
Ru–C–O(av)	175(1)	Ru–C–O(av)	175(1)	Ru–C–O(av)	175(1)

[a] Estimated S.D.s in the least significant figure are given in parentheses.

atoms, one platinum and five ruthenium, with a carbido carbon atom in the center. There is an MPh_2 group bridging one of the Pt–Ru bonds in the site analogous to that of the bridging carbonyl ligand in **1**. The Pt–Ru bond distances in all three compounds are similar, and similar to that of **1** [23]. As expected, the Pt–Ge and Ru–Ge distances (Pt(1)–Ge(1) = 2.4701(6) Å, Ru(1)–Ge(1) = 2.4457(8) Å) are slightly shorter than the Pt–Sn and Ru–Sn distances (Pt(1)–Sn(1) = 2.6314(6) Å, Ru(1)–Sn(1) = 2.6074(7) Å), which are in turn slightly shorter than the Pt–Pb and Ru–Pb distances (Pt(1)–Pb(1) = 2.7037(3) Å, Ru(1)–Pb(1) = 2.6668(5) Å). The Pt–M distances are slightly larger than the Ru–M distances. The Ru–Ge bond distance in **4** is slightly shorter than those found for the bridging $GePh_2$ ligands in the compounds $Ru_5(CO)_{11}(\mu\text{-}CO)(\mu\text{-}GePh_2)_3(\mu_5\text{-}C)$ (range: 2.4792(7)–2.5166(6) Å) and $Ru_5(CO)_{11}(\mu\text{-}GePh_2)_4(\mu_5\text{-}C)$ (range: 2.4732(11)–2.5133(12) Å) [24]. The Ru–Sn distance in **5** is similar to the shortest distances found for the bridging $SnPh_2$ ligands in the compounds $Ru_5(CO)_8(\mu\text{-}SnPh_2)_4(C_6H_6)(\mu_5\text{-}C)$ (range: 2.6022(12)–2.6654(12) Å) and $Ru_5(CO)_7(\mu\text{-}SnPh_2)_4(SnPh_3)(C_6H_6)(\mu_5\text{-}C)(\mu\text{-}H)$ (range: 2.6125(8)–2.7106(8) Å) [25]. The Ru–Pb distances in **6** are slightly shorter than those in the compound $Ru_3[\mu\text{-}Pb\{CH(SiMe_3)_2\}_2]_2(\mu\text{-}CO)(CO)_9$ [32], which range from 2.767(2) to 2.790(2) Å. The longer distances in $Ru_3(\mu\text{-}[Pb\{CH(SiMe_3)_2\}_2])(\mu\text{-}CO)(CO)_9$ may be a consequence of steric interactions between the bulky $\{CH(SiMe_3)_2\}$ groups on the Pb atoms, and the CO ligands on the ruthenium atoms.

It is proposed that the reactions of **1** with Ph_3GeH and Ph_3SnH proceed by CO elimination from **1** and an oxidative addition of the M–H bond to the cluster to yield some unobserved intermediate containing an $SnPh_3$ group and a hydride ligand. We have shown previously that the reactions of Ph_3SnH with $Ru_5(CO)_{15}(\mu_5\text{-}C)$ proceed by just such a process [25]. Based on the following evidence we believe that this first step probably involves the platinum atom: (1) the

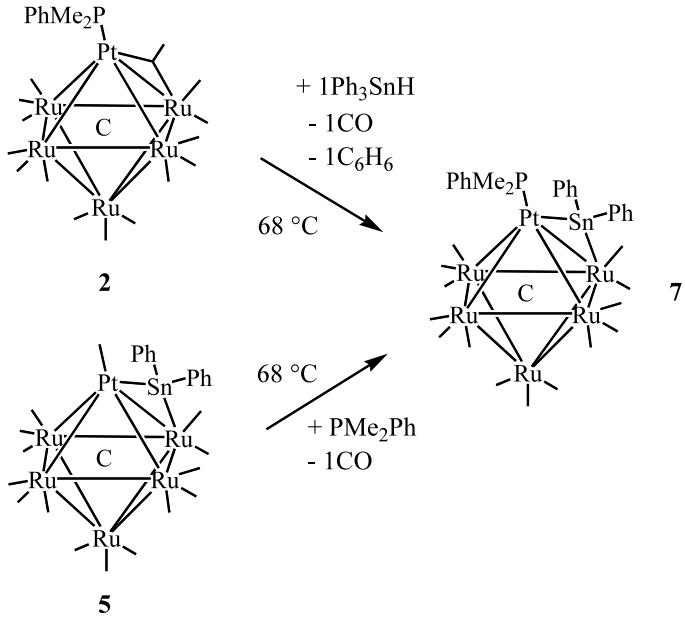

Scheme 1.

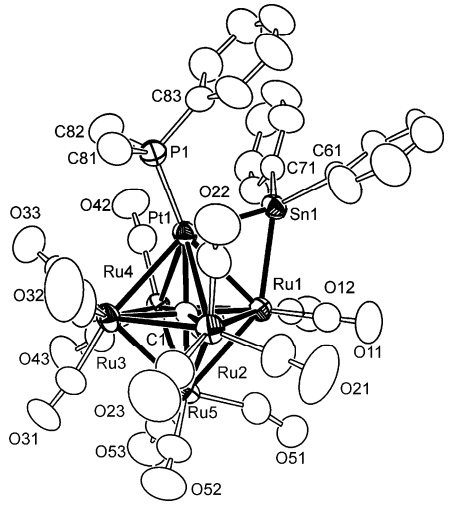

Fig. 2. An ORTEP diagram of the molecular structure of $PtRu_5(CO)_{14}(\mu\text{-}SnPh_2)(PMe_2Ph)(\mu_6\text{-}C)$ (**7**) showing 40% thermal ellipsoid probability.

bridging MPh_2 groups are bonded to the platinum atom, and (2) the reaction of **1** with Ph_3SnH occurs at a much lower temperature than that of the reaction of its platinum-free parent $Ru_5(CO)_{15}(\mu_5\text{-}C)$. Subsequently, a phenyl group is cleaved from the $SnPh_3$-containing

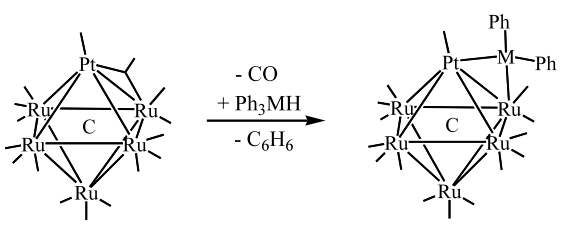

(1)

Table 4
Selected intramolecular distances and angles for $PtRu_5(CO)_{14}(P\text{-}Me_2Ph)(\mu\text{-}SnPh_2)(\mu_6\text{-}C)$ (**7**) [a]

Atom	Distance (Å)
Ru(1)–Pt(1)	2.9107(5)
Ru(1)–Ru(2)	2.9498(7)
Ru(1)–Ru(4)	2.9386(6)
Ru(1)–Ru(5)	2.9016(6)
Ru(2)–Pt(1)	2.9405(6)
Ru(2)–Ru(3)	2.8823(7)
Ru(2)–Ru(5)	2.8468(8)
Ru(3)–Pt(1)	2.8831(5)
Ru(3)–Ru(4)	2.8380(7)
Ru(3)–Ru(5)	2.9007(7)
Ru(4)–Ru(5)	2.8315(6)
Pt(1)–Sn(1)	2.5825(6)
Ru(1)–Sn(1)	2.6590(6)
Pt(1)–P(1)	2.2476(14)
Pt(1)–C(1)	2.039(5)
Ru(1)–C(1)	2.035(5)
Ru(2)–C(1)	2.049(5)
Ru(3)–C(1)	2.065(5)
Ru(4)–C(1)	2.062(5)
Ru(5)–C(1)	2.061(5)
C–O(av)	1.13(1)
Atom	**Angle (°)**
Ru(1)–Pt(1)–Ru(3)	90.084(14)
Ru(1)–Pt(1)–Sn(1)	57.529(13)
P(1)–Pt(1)–Ru(1)	156.26(4)
Pt(1)–Ru(1)–Sn(1)	55.023(12)
Pt(1)–Sn(1)–Ru(1)	67.448(15)
Ru(1)–Ru(5)–Ru(3)	89.917(17)
Ru(4)–Ru(5)–Ru(2)	92.555(17)
Pt(1)–Ru(1)–Ru(5)	89.705(15)
Pt(1)–Ru(3)–Ru(5)	90.268(16)
Ru(4)–Ru(1)–Ru(2)	88.360(17)
Ru(4)–Ru(3)–Ru(2)	91.676(18)
Ru–C–O(av)	170(1)

[a] Estimated S.D.s in the least significant figure are given in parentheses.

intermediate, which then combines with the hydride ligand to yield the observed products (Eq. (1)).

The reaction of **1** with Pb_2Ph_6 may involve some similar species, but the fate of the eliminated phenyl group was not ascertained in this reaction.

The phosphine derivative of **1**, $PtRu_5(CO)_{15}(P\text{-}Me_2Ph)(\mu_6\text{-}C)$ (**2**), reacted with Ph_3SnH at 68 °C to afford the cluster complex $PtRu_5(CO)_{14}(\mu\text{-}SnPh_2)\text{-}(PMe_2Ph)(\mu_6\text{-}C)$ (**7**) in 20% yield which is the PMe_2Ph derivative of **5**. Compound **7** can be obtained in a better yield (41%) simply by the treatment of **5** with PMe_2Ph (see Scheme 1). Compound **7** was also characterized by a combination of IR, NMR, and single crystal X-ray diffraction analyses. An ORTEP diagram of the molecular structure of **7** is shown in Fig. 2. Selected bond distances and angles are listed in Table 4. Like **4**–**6**, compound **7** also consists of an octahedral cluster containing one platinum and five ruthenium atoms,

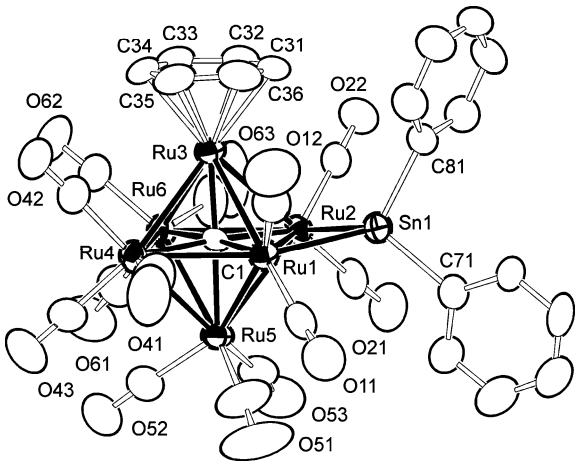

Fig. 3. An ORTEP diagram of the molecular structure of $Ru_6(CO)_{13}(\mu\text{-}SnPh_2)(\eta^6\text{-}C_6H_6)(\mu_6\text{-}C)$ (**8**) showing 40% thermal ellipsoid probability.

and a single carbon atom in the center. The PMe_2Ph ligand is terminally coordinated to the platinum atom and the $SnPh_2$ group has replaced the bridging carbonyl ligand between Pt(1) and Ru(1) in **2**. The Pt–Ru bond distances that lie in the range 2.8831(5)–2.9863(6) Å are similar to those in **4**–**6**. The Pt–Sn distance of 2.5825(5) Å is shorter than the Pt–Sn distance in **5**, 2.6314(6) Å. This is contrary to what one would expect on the basis of steric considerations, so it must be an electronic effect. Replacement of the CO ligand in **5** with the poorer acceptor PMe_2Ph should lead to an increase in electron density on the platinum atom. This could result in better orbital overlaps between the platinum and tin atoms and result in a stronger and shorter platinum–tin bond.

Table 5
Selected intramolecular distances and angles for $Ru_6(CO)_{13}(\eta^6\text{-}C_6H_6)(\mu\text{-}SnPh_2)(\mu_6\text{-}C)$ (**8**) [a]

Atom	Distance (Å)
Ru(1)–Ru(2)	3.016(1)
Ru(1)–Ru(3)	2.905(1)
Ru(1)–Ru(4)	2.886(1)
Ru(1)–Ru(5)	2.973(1)
Ru(2)–Ru(3)	2.886(1)
Ru(2)–Ru(5)	2.916(1)
Ru(2)–Ru(6)	2.977(1)
Ru(3)–Ru(4)	2.881(1)
Ru(3)–Ru(6)	2.839(1)
Ru(4)–Ru(5)	2.870(1)
Ru(4)–Ru(6)	2.883(1)
Ru(5)–Ru(6)	2.857(1)
Ru(1)–Sn(1)	2.626(1)
Ru(2)–Sn(1)	2.622(1)
Ru(3)–C(31)	2.23(1)
Ru(3)–C(33)	2.27(1)
Ru(3)–C(34)	2.24(1)
Ru(3)–C(35)	2.22(1)
Ru(3)–C(36)	2.26(1)
C–O(av)	1.15(1)
Atom	**Angle (°)**
Ru(1)–Sn(1)–Ru(2)	70.15(3)
Ru(1)–Ru(3)–Ru(6)	92.89(3)
Ru(2)–Ru(3)–Ru(4)	92.06(3)
Ru(2)–Ru(1)–Ru(4)	89.37(3)
Ru(3)–Ru(1)–Ru(5)	86.19(3)
Sn(1)–Ru(2)–Ru(3)	91.93(3)
Sn(1)–Ru(1)–Ru(3)	91.42(3)
Ru(1)–C(1)–Ru(6)	174.8(4)
Ru(3)–C(1)–Ru(5)	177.2(5)
Ru–C–O(av)	170(1)

[a] Estimated S.D.s in the least significant figure are given in parentheses.

The reaction of Ph_3SnH with the hexaruthenium cluster $Ru_6(CO)_{14}(\eta^6\text{-}C_6H_6)(\mu_6\text{-}C)$ (**3**) at room temperature gave the $SnPh_2$ derivative $Ru_6(CO)_{13}(\mu\text{-}SnPh_2)(\eta^6\text{-}C_6H_6)(\mu_6\text{-}C)$ (**8**) in 10% yield. Compound **8** was characterized by a combination of IR, NMR, and single crystal X-ray diffraction analyses. An ORTEP diagram of the molecular structure of **8** is shown in Fig. 3. Selected bond distances and angles are listed in Table 5. Compound **8** consists of an Ru_6 octahedron with a carbon atom in the center. There is an η^6-benzene ligand coordinated to one of the ruthenium atoms, Ru(3), and an $SnPh_2$ group bridging the ruthenium–ruthenium bond, Ru(1)–Ru(2). Formally, the bridging $SnPh_2$ group has replaced the bridging CO ligand in **3** (see Eq. (2)). The Ru(1)–Sn(1) and Ru(2)–Sn(1) bond distances of 2.626(1) and 2.622(1) Å, respectively, are similar to the Ru–Sn distances found in **5** and **7**.

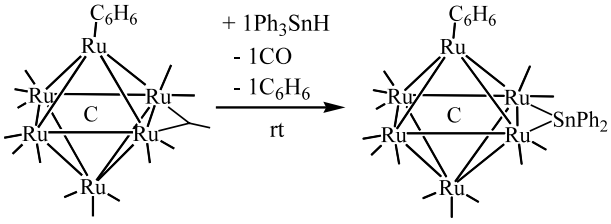

3 **8** (2)

4. Summary

In this work, we have expanded the realm of reactions that provide transition metal cluster complexes containing bridging MPh_2 ligands, M = Ge, Sn, Pb, but unlike our previous studies with $Ru_5(CO)_{15}(\mu_6\text{-}C)$ we have not observed any evidence for the formation of hexanuclear metal complexes containing more than one MPh_2 ligand. Also, we have not yet succeeded in preparing complexes containing bridging $SiPh_2$ ligands by cleavage of phenyl groups from $SiPh_3$ precursors. It seems likely that suitable treatment of these new compounds could

provide trimetallic nanoparticles that might exhibit useful properties as catalysts [4].

5. Supplementary material

Crystallographic data for the structural analysis have been deposited with the Cambridge Crystallographic Data Centre, CCDC Nos. 199367–199371 for compounds **4**–**8**, respectively. Copies of this information may be obtained free of charge from The Director, CCDC, 12 Union Road, Cambridge CB2 1EZ, UK (Fax: +44-1223-336033; e-mail: deposit@ccdc.cam.ac.uk or www: http://www.ccdc.cam.ac.uk).

Acknowledgements

These studies were supported by the Division of Chemical Sciences of the Office of Basic Energy Sciences of the US Department of Energy under Grant No. DE-FG02-00ER14980 and the USC Nanocenter.

References

[1] N. Toshima, T. Yonezawa, New J. Chem. 11 (1998) 1179.
[2] B.F.G. Johnson, Coord. Chem. Rev. 192 (1999) 1269.
[3] P.A. Midgley, M. Weyland, J.M. Thomas, B.F.G. Johnson, Chem. Commun. (2001) 907.
[4] M.S. Nashner, A.I. Frenkel, D. Somerville, C.W. Hills, J.R. Shapley, R.G. Nuzzo, J. Am. Chem. Soc. 120 (1998) 8093.
[5] M.S. Nashner, A.I. Frenkel, D.L. Adler, J.R. Shapley, R.G. Nuzzo, J. Am. Chem. Soc. 119 (1997) 7760.
[6] D.S. Shephard, T. Maschmeyer, B.F.G. Johnson, J.M. Thomas, G. Sankar, D. Ozkaya, W. Zhou, R.D. Oldroyd, R.G. Bell, Angew. Chem. Int. Ed. 36 (1997) 2242.
[7] R. Raja, G. Sankar, S. Hermans, D.S. Shephard, S. Bromley, J.M. Thomas, B.F.G. Johnson, Chem. Commun. (1999) 1571.
[8] (a) R. Raja, T. Khimyak, J.M. Thomas, S. Hermans, B.F.G. Johnson, Angew. Chem. Int. Ed. 40 (2001) 4639;
(b) D.S. Shephard, T. Maschmeyer, G. Sankar, J.M. Thomas, D. Ozkaya, B.F.G. Johnson, R. Raja, R.D. Oldroyd, R.G. Bell, Chem. Eur. J. 4 (1998) 1214.
[9] J.H. Sinfelt, Bimetallic Catalysts: Discoveries, Concepts and Applications, Wiley, New York, 1983.
[10] N. Macloed, J.R. Frer, D. Stirling, G. Webb, Catal. Today 46 (1998) 37.
[11] A.C. Muller, P.A. Engelhard, J.E. Weisang, J. Catal. 56 (1979) 65.
[12] Z. Bodnar, T. Mallat, I. Bakos, Appl. Catal. A 102 (1993) 105.
[13] R. Schlogl, K. Noack, H. Zbinden, Helv. Chim. Acta 70 (1987) 627.
[14] (a) S. Hermans, R. Raja, J.M. Thomas, B.F.G. Johnson, G. Sankar, D. Gleeson, Angew. Chem. Int. Ed. 40 (2001) 1211;
(b) S. Hermans, B.F.G. Johnson, Chem. Commun. (2000) 1955.;
(c) R. Raja, T. Khimyak, J.M. Thomas, S. Hermans, B.F.G. Johnson, Angew. Chem. Int. Ed. 40 (2001) 4638.
[15] A. Tijani, B. Coq, F. Figueras, Appl. Catal. 76 (1991) 255.
[16] M.C. Sanchez-Sierra, J. García-Ruiz, M.G. Proietti, J. Blasco, J. Mol. Catal. A 108 (1996) 95.
[17] W.A. Hermann, Angew. Chem. Int. Ed. 25 (1986) 56.
[18] K.H. Whitmire, J. Coord. Chem. 17 (1988) 95.
[19] N.A. Compton, R.J. Errington, N.C. Norman, Adv. Organomet. Chem. 31 (1990) 91.
[20] W.K. Leong, W.B. Fredrick, W.B. Einstein, R.K. Pomeroy, Organometallics 15 (1996) 1589.
[21] J. Howard, P. Woodward, J. Chem. Soc. A (1971) 3648.
[22] R. Ball, J.M. Bennett, Inorg. Chem. 11 (1972) 1806.
[23] Y. Zhang, B. Wang, S. Xu, X. Zhou, Organometallics 20 (2001) 3829.
[24] R.D. Adams, B. Captain, W. Fu, Inorg. Chem., 42 (2003) 1328.
[25] (a) R.D. Adams, B. Captain, W. Fu, M.D. Smith, Inorg. Chem. 41 (2002) 5593;
(b) R.D. Adams, B. Captain, W. Fu, M.D. Smith, Inorg. Chem. 41 (2002) 2302.
[26] R.D. Adams, W. Wu, J. Cluster Sci. 2 (1991) 271.
[27] R.D. Adams, B. Captain, W. Fu, P.J. Pellechia, Chem. Commun. (2000) 937.
[28] P.J. Dyson, B.F.G. Johnson, J. Lewis, M. Martinelli, D. Braga, F. Grepioni, J. Am. Chem. Soc. 115 (1993) 9062.
[29] (a) International Tables for X-ray Crystallography, Vol. IV, Kynoch, Birmingham, UK, 1975, pp. 99–101 (Table 2.2B).;
(b) International Tables for X-ray Crystallography, Vol. IV, Kynoch, Birmingham, UK, 1975, pp. 149–150 (Table 2.3.1).
[30] SAINT+, version 6.02a, Bruker Analytical X-ray System, Inc., Madison, WI, 1998.
[31] G.M. Sheldrick, SHELXTL, version 5.1, Bruker Analytical X-ray Systems, Inc, Madison, WI, 1997.
[32] N.C. Burton, C.J. Cardin, D.J. Cardin, B. Twamley, Y. Zubavichus, Organometallics 14 (1995) 5708.